Supporting Information

High-entropy modulated polarization evolution for enhanced pyroelectric performance in BNT ceramics

Xiaofei Su, Liguang Wang*, Changming Zhu**, Guibo Yu, Xinlin Jiang, Na Shen, Maoying Qin, Xiaoxuan Zheng, Yu Wang, Houbing Zhou

College of Physics and Technology, Guangxi Normal University & University Engineering Research Center of Advanced Functional Materials and intelligent sensing, Guangxi, Guilin 541004, People's Republic of China

* Corresponding author. E-mail address: wangliguang@gxnu.edu.cn (Liguang Wang*)

zhuchangming@gxnu.edu.cn (Changming Zhu**)

Characterization Methods

The phase structures of the samples were examined by X-ray diffraction (XRD, Rigaku Miniflex 600) using Cu Kα radiation with a wavelength of 1.5406 Å. The measurements were carried out with a step size of 0.01° and a scanning rate of 1°/min. Fracture surfaces and surface morphologies were observed using a field-emission scanning electron microscope (FE-SEM, FEI Quanta 200). Local structural evolution was further investigated by confocal micro-Raman spectroscopy (LabRAM HR Evolution, Horiba) with a 532 nm laser as the excitation source. The obtained XRD patterns were refined using the Rietveld method to extract detailed phase-structure information and phase coexistence features.

Dielectric properties were measured using a PEMS 6000 (Balab) system in the frequency range from 1 kHz to 100 kHz. Ferroelectric hysteresis loops and electric-field-induced strain behaviors were recorded using a Radiant Precision Premier II system equipped with an MTI-2100 Fotonic Sensor. The piezoelectric coefficient d_{33} was measured using a quasi-static d_{33} meter (Type ZJ-3AN, Institute of Acoustics). Pyroelectric properties were evaluated using a RMS-1000I (Balab) thermoelectric material testing system. The pyroelectric current during heating and cooling processes was collected using a Keithley 6517B electrometer. The specific heat capacity was determined using differential scanning calorimetry (DSC-214, NETZSCH), and the obtained data were employed to calculate the piezoelectric

activity quality factors. The bulk density of the sintered ceramics was measured using the Archimedes technique to evaluate their densification. The domain configurations and switching dynamics were examined using piezoresponse force microscopy (PFM, Bruker Dimension Icon) under an in situ bias of 10 V.

Table S1. Calculated configurational entropy values of the (1-*x*)BNT-*x*BNBTGS ceramics with different contents.

x	0	0.06	0.08	0.10	0.12	0.14	0.16	0.18	0.20
S_{config}	0.69*R*	0.84*R*	0.88*R*	0.91*R*	0.95*R*	0.98*R*	1.01*R*	1.03*R*	1.06*R*

Figures

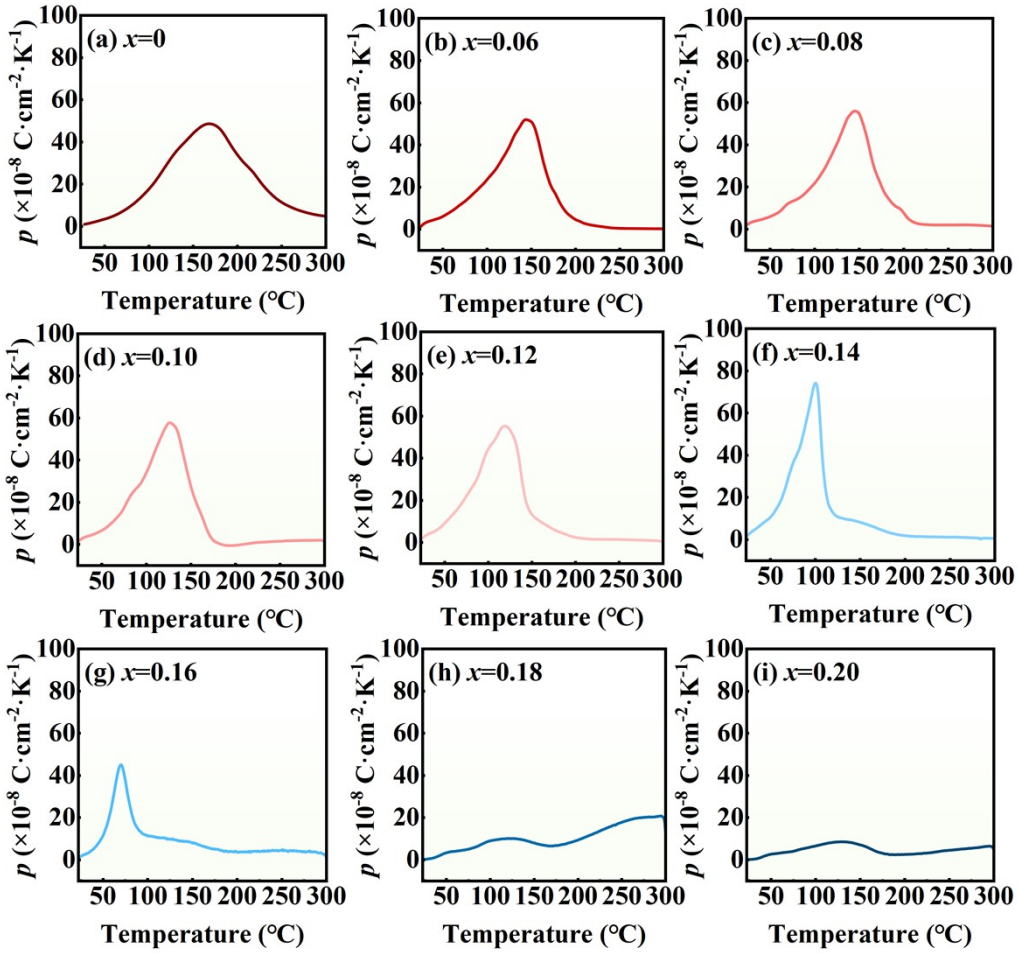

Fig. S1. (a-i) Temperature dependent pyroelectric coefficient (*p*) for (1-*x*)BNT-*x*BNBTGS ceramics with *x*=0-0.20.

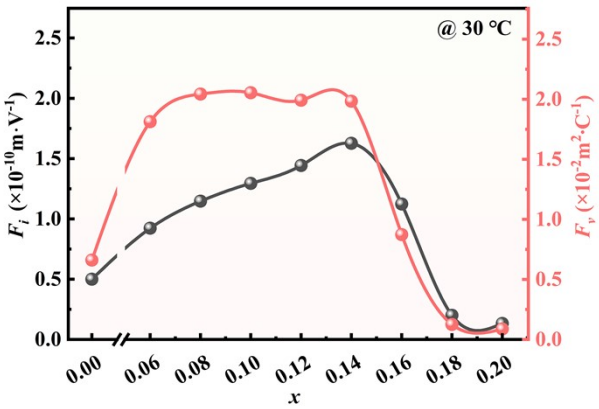

Fig. S2. Composition dependence of the pyroelectric figures of merit F_i and F_v for samples with x=0-0.20.

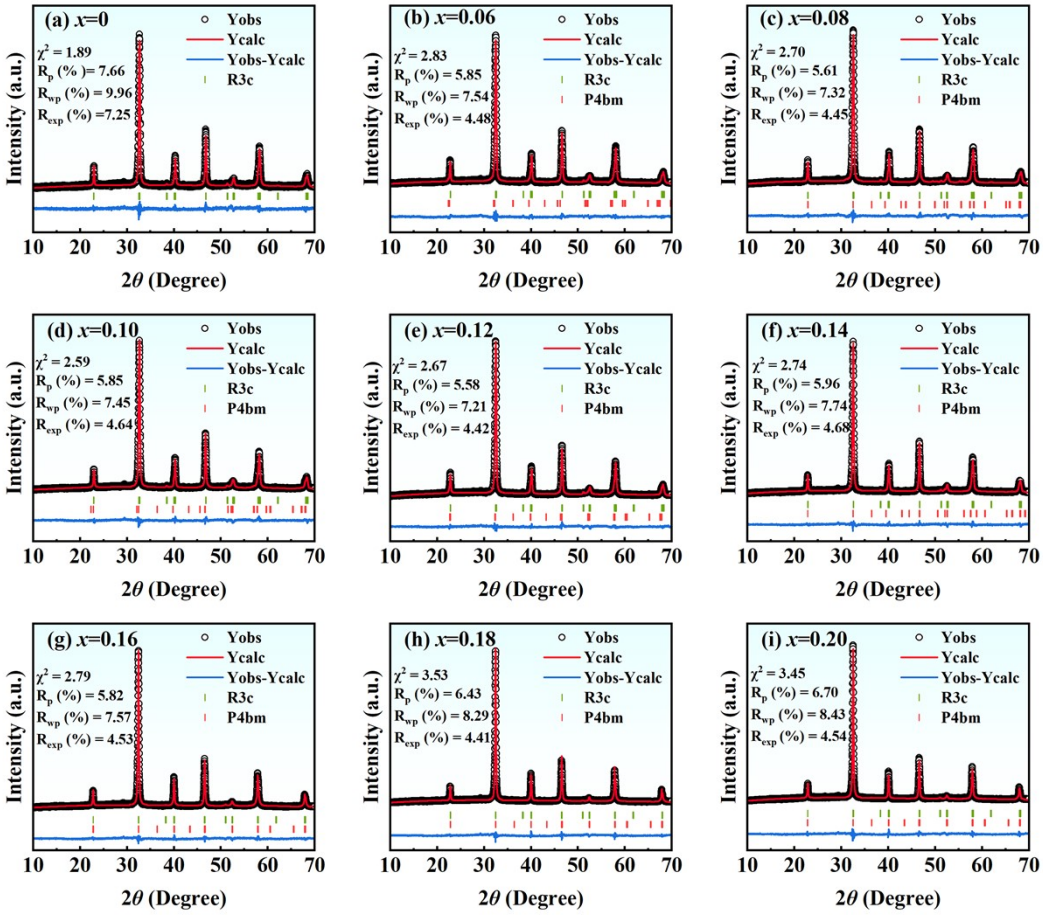

Fig. S3. (a-i) Rietveld-refined XRD patterns and corresponding fitting parameters for (1-x)BNT-xBNBTGS ceramics with x=0-0.20 measured at room temperature.

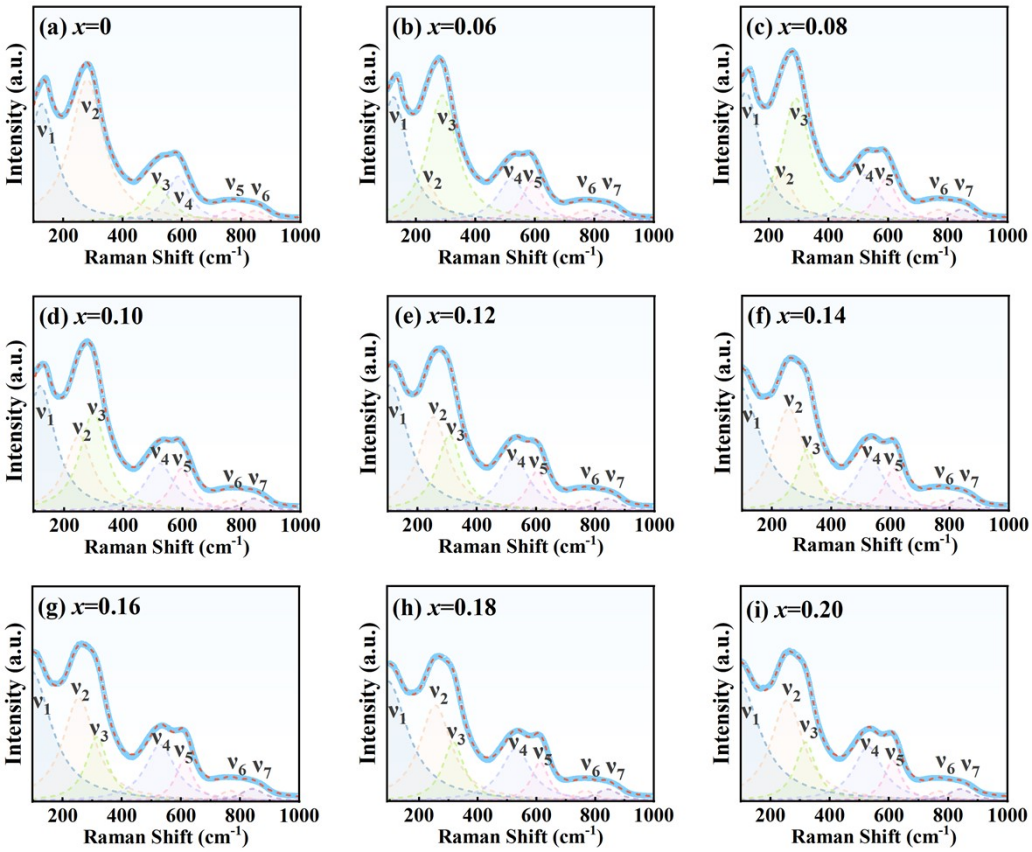

Fig. S4. (a-i) Lorentzian peak fitting and decomposition of Raman spectra for (1-*x*)BNT-*x*BNBTGS ceramics (*x*=0-0.20).

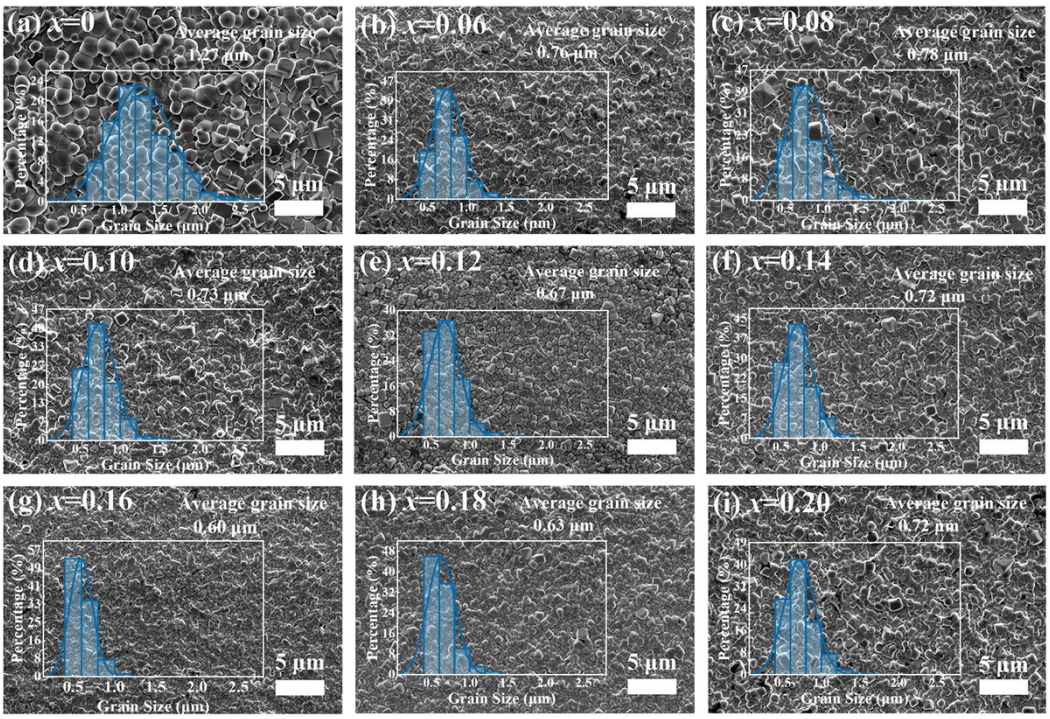

Fig. S5. (a-i) SEM images of (1-*x*)BNT-*x*BNBTGS ceramics with different compositions measured at room temperature. Insets show the corresponding grain size distributions and average grain sizes.

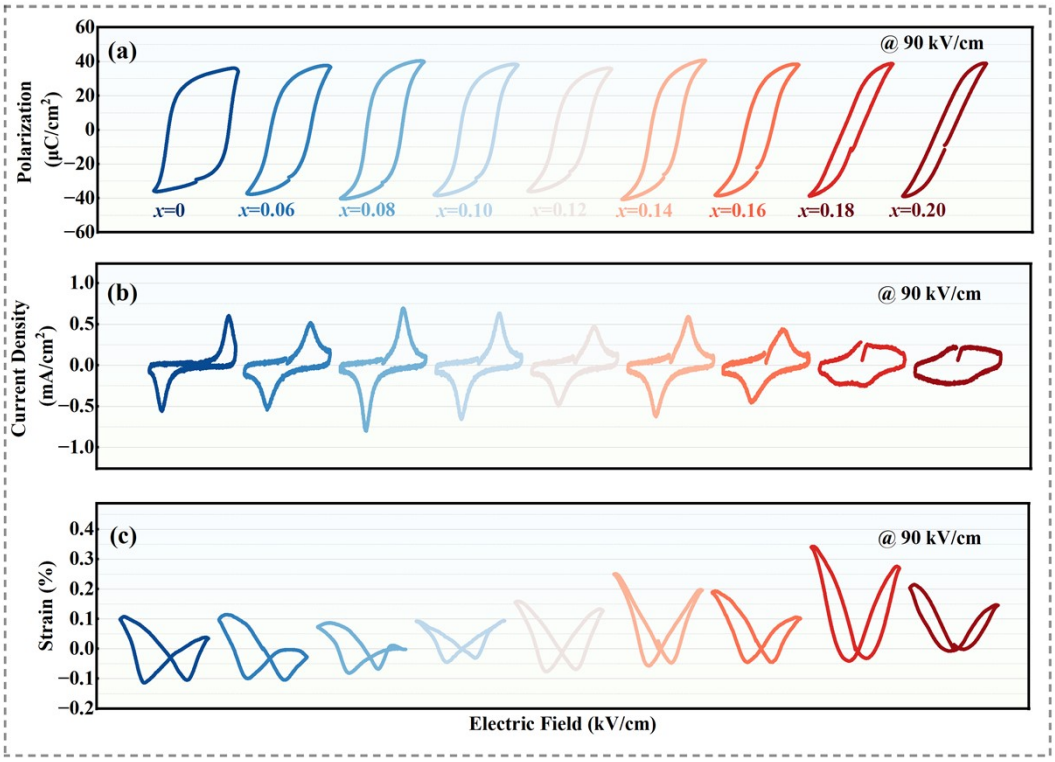

Fig. S6. Room-temperature ferroelectric and strain performance of (1-*x*)BNT-*x*BNBTGS ceramics with *x*=0-0.20. (a) Polarization-electric field hysteresis loops measured at 90 kV/cm. (b) Corresponding current density curves measured at 90 kV/cm. (c) Bipolar strain-electric field curves measured at 90 kV/cm.